Research Article

Minhui Yang#, Hualan Zhou#, Yuxin Cheng, Qingxiang Hong, Jie Chen, Qiuyang Zhang*, and Changjiang Pan*

Incorporation of copper and strontium ions in TiO_2 nanotubes *via* dopamine to enhance hemocompatibility and cytocompatibility

https://doi.org/10.1515/ntrev-2022-0090
received January 24, 2022; accepted March 9, 2022

Abstract: Nanomaterials with unique nanotube arrays have attracted extensive attention in the field of blood-contacting biomaterials. In this study, the regular titanium dioxide nanotube arrays were first prepared on the pure titanium surface by anodic oxidation. Subsequently, copper ions (Cu^{2+}) and strontium ions (Sr^{2+}) were incorporated into the nanotubes by the chelation of dopamine to improve biocompatibility. The as-prepared TiO_2 nanotubes had an inner diameter of about 60 nm and an outer diameter of 90–110 nm, as well as a tube length of 4–6 μm. The following annealing treatment and the incorporation of Cu^{2+} and Sr^{2+} had little effect on the morphology and dimensions of the nanotubes, but can significantly improve the hydrophilicity, and promote the adsorption of bovine serum albumin concurrently inhibit the adsorption of fibrinogen, showing the effect of selective protein adsorption. At the same time, loading Cu^{2+} and Sr^{2+} can also effectively inhibit platelet adhesion and activation, promote endothelial cell growth, and upregulate the expression of vascular endothelial growth factor and nitric oxide. Therefore, the results of this study showed that the incorporation of Cu^{2+} and Sr^{2+} into the TiO_2 nanotubes can simultaneously improve the hemocompatibility and cytocompatibility of endothelial cells, which can enlarge the application of titanium-based biomaterials in cardiovascular devices such as a stent.

Keywords: titanium dioxide nanotubes, copper ions, strontium ions, blood compatibility, cell compatibility

1 Introduction

Cardiovascular disease has the characteristics of high prevalence, disability, and mortality, which seriously threatens human health around the world. In addition to drug administration and surgical treatment, stent insertion has become one of the main approaches to treat stenotic cardiovascular disease [1]. Titanium-based biomaterials have excellent mechanical properties and corrosion resistance in the physiological environment, and they are good candidates for cardiovascular implant materials. However, the bioactivities of the titanium surface are limited and it could easily cause surface thrombosis and endothelial dysfunction after the implantation [2]. It has been found that the materials with micro-nano surface structure have outstanding performances in promoting cell growth and improving blood biocompatibility. For example, the titanium dioxide nanotube (TNT) array has the advantages of the high specific surface area, controllable tube diameter and length, and the ability to load bioactive factors, to improve the biocompatibility. It has great potential for application in cardiovascular implant materials [3]. The nanotube array *in situ* prepared on the

# These authors contributed equally to this work.

*** Corresponding author: Qiuyang Zhang,** Faculty of Mechanical and Material Engineering, Jiangsu Provincial Engineering Research Center for Biomaterials and Advanced Medical Devices, Huaiyin Institute of Technology, Huai'an 223003, China, e-mail: qyzhang@hyit.edu.cn
*** Corresponding author: Changjiang Pan,** Faculty of Mechanical and Material Engineering, Jiangsu Provincial Engineering Research Center for Biomaterials and Advanced Medical Devices, Huaiyin Institute of Technology, Huai'an 223003, China, e-mail: panchangjiang@hyit.edu.cn
Minhui Yang, Yuxin Cheng, Qingxiang Hong, Jie Chen: Faculty of Mechanical and Material Engineering, Jiangsu Provincial Engineering Research Center for Biomaterials and Advanced Medical Devices, Huaiyin Institute of Technology, Huai'an 223003, China
Hualan Zhou: The Affiliated Huai'an Hospital of Xuzhou Medical University, Huai'an 223003, China

titanium surface not only keeps the good mechanical properties and corrosion resistance of the titanium itself but also establishes a unique micro-nano structure on the surface, leading to the improvement of biocompatibility [4]. Anodic oxidation represents one of the simple and cost-effective methods to *in situ* prepare regular nanotube arrays with the different tube diameters and lengths on the titanium surface [5]. Loading various bioactive substances into the nanotubes can further significantly improve biocompatibility [6–8].

Studies have shown that copper (Cu) plays an important role in the physiological processes of cells. As a cofactor of various enzymes, it is distributed in different organelles of cells, such as mitochondria, nuclei, and lysosomes [9,10]. Cu has been proved to have a variety of biological functions. The introduction of Cu^{2+} on the biomaterial surface can not only improve anticoagulation and promote angiogenesis [11] but also enhance the activity and proliferation of the endothelial cells by upregulating the expression of vascular endothelial factors, to accelerate endothelialization [12]. Therefore, loading Cu^{2+} into TNT can significantly improve hemocompatibility and promote the growth of endothelial cells. At the same time, strontium (Sr) is also an essential trace element in the human body. In the body, the level of Sr is closely related to vascular diseases [13], and Sr deficiency leads to vascular diseases such as vascular injury and arteriosclerosis of the central nervous system [14]. In addition, Sr has the function of promoting angiogenesis [15]. A recent study indicated that Sr can promote the early vascularization of biomaterials by regulating the microvascular phenotype [16]. In addition, Sr can promote the migration, proliferation, and angiogenesis-related ribonucleic acid (RNA) expression of human vascular endothelial cells [17]. However, there are still a few reports exploring the effects of Sr^{2+} on blood compatibility and endothelial cell behaviors.

In this study, based on the application potentials of TNT, Cu, and Sr in the cardiovascular biomaterials, TNT were *in situ* prepared on the pure titanium surface by anodic oxidation and then annealed to obtain anatase nanotube arrays. Finally, Cu^{2+} and Sr^{2+} were incorporated into the nanotubes by the chelation with metal ions and the self-polymerization of dopamine (Dopa) on the surface. The results showed that the TNT incorporated with Cu^{2+} and Sr^{2+} can significantly improve blood compatibility and promote endothelial cell growth through the sustainable release of Cu^{2+} and Sr^{2+}.

2 Materials and methods

2.1 Preparation of TNT

TNT arrays were prepared according to our previous method [18]. The oxidation was carried out with a titanium sheet as anode and graphite rod as the cathode. The electrolyte was ethylene glycol containing 0.5 wt% NH_4F and 2 vol% H_2O. The voltage was 45 V and the current was 3 A. The samples were taken out after 1 h anodization, and they were ultrasonically cleaned with ethylene glycol and ethanol for 5 min, respectively. After being dried, they were annealed at 450°C in the box resistance furnace (AY-BY-145) for 2.5 h to obtain the annealed TiO_2 nanotubes (TNTA).

2.2 Loading Cu^{2+} and Sr^{2+} *via* dopamine

First, 50 mL of 2 mg/mL dopamine solution (Tris HCl buffer, 0.01 M, pH 8.5) was prepared and then 100 mg of $CuCl_2$ was added to the solution. The TNTA samples were immersed into the solution for reacting 12 h. After being washed with deionized water and dried, the samples were immersed into 50 mL dopamine (2 mg/mL) solution with the different feed of Sr $(OH)_2$. The additional amount of Sr $(OH)_2$ was calculated according to Cu:Sr atomic ratio of 1:0.5, 1:1, and 1:2. After being washed and dried, three groups of TNT incorporated with the different ratios of Cu^{2+} and Sr^{2+} were obtained (TNTA–Dopa–Cu–Sr0.5, TNTA–Dopa–Cu–Sr1 and TNTA–Dopa–Cu–Sr2). As a control, the TNTA sample was immersed into the above dopamine solution to prepare the dopamine-modified TiO_2 nanotubes (TNTA–Dopa).

2.3 Surface characterization

The morphologies and dimensions of different nanotubes were examined by scanning electron microscopy (SEM, FEI Quanta250). The element distribution and content on the surface were analyzed by energy dispersive spectrum (EDS, IMA X-Max 20, Britain). To further observe the cross-sectional morphology and element distribution, the sample was cut and observed by SEM and EDS. X-ray diffraction (X-ray Diffraction, Switzerland,

SCINTXTRA) was used to investigate the crystal structural changes on the titanium surface, and the scanning range was 15–85°. The surface hydrophilicity was characterized by water contact angle measurement (DSA25, KrüssGmbH, Germany). Three parallel samples were measured at room temperature and the values were averaged.

2.4 The release profiles of Cu^{2+} and Sr^{2+}

The TNT array samples loaded with Cu^{2+} and Sr^{2+} were immersed into 5 mL phosphate buffer solution (PBS) solution (pH 7.4) at 37°C for 14 days. At different intervals, 500 µL PBS was taken out for the measurement and 500 µL fresh PBS solution was supplemented. The release concentrations of Cu^{2+} and Sr^{2+} were measured using an inductively coupled plasma emission spectrometer (Optima 7000 DV, USA). The release curves were plotted according to the standard curves.

2.5 Protein adsorption

Bicinchoninic acid (BCA) Protein Assay Kit (Shenzhen Ziker Biological Technologies Co., Ltd) was used to measure the adsorption behaviors of bovine serum albumin (BSA) and fibrinogen (FIB) on the surfaces. First 1 mg/mL of BSA and FIB solution (in 0.01 M PBS) were prepared. The samples were equilibrated with PBS solution for 2 h, and then immersed in 2 mL protein solution at 37°C for 3 h. After being rinsed three times by PBS, they were immersed in 2 mL of sodium dodecyl sulfate (SDS, 1 wt%) solution, and then ultrasonically cleaned for 30 min. 100 µL eluent and 100 µL BCA working solution (reagent A:reagent B = 50:1) were mixed for reacting 20 min at 37°C, and then 200 µL of the reaction liquid was transferred into a 96-well plate to measure the absorbance at 562 nm using a Microplate Reader (Bio-Tek, Eons), and the protein adsorption amount was calculated according to the standard curve.

2.6 Blood compatibility

2.6.1 Platelet adhesion and activation

The fresh human whole blood containing anticoagulant was centrifuged for 10 min at 1,200 rpm to obtain the platelet-rich plasma (PRP). Nearly, 200 µL of PRP was dropped on each sample surface and incubated for 2 h at 37°C. Afterward, the samples were washed twice with normal saline and then fixed at 4°C by 2.5% glutaraldehyde solution (prepared with normal saline) for 3 h. After being successively dehydrated by 50, 70, 90, and 100% ethanol solutions for 15 min each, the samples were dried at room temperature. The number and morphologies of the attached platelets were observed by SEM (FEI Quanta250).

Enzyme-linked immunosorbent assay kit (ELISA; Shanghai Enzyme-Linked Biotechnology Co., Ltd) was used to determine the platelet activation by measuring the released GMP140 of the attached platelets. Each sample was covered by 50 µL PRP and then cultured at 37°C for 2 h. In a 96-well plate, 40 µL diluent and 10 µL cultured PRP were mixed, followed by adding 100 µL enzyme-labeled reagent. The mixed solution was incubated for 1 h at 37°C. After being washed five times, the chromogenic agent was added and kept away from light for 15 min at 37°C. Finally, 50 µL termination solution was added to each well to terminate the reaction. The absorbance was measured at 450 nm, and the amount of the platelet activation was calculated according to the standard curve.

2.6.2 Hemolysis rate (HR)

The human blood from a healthy volunteer was centrifuged for 10 min at 1,200 rpm to collect the erythrocytes for hemolysis assay. The red blood cells were prepared into 2% suspension with 0.9% NaCl solution. 2 mL suspension was added to each sample and incubated for 3 h at 37°C. About 1 mL of red blood cell solution was taken out from each sample to centrifuge for 5 min at 3,000 rpm. 200 µL supernatant was transferred into a 96-well plate for measuring the absorbance at 450 nm. The 2% red blood cells were separately dissolved into the distilled water and physiological saline as the positive control (D1) and negative control (D2). The average value was taken from multiple measurements, and then the HR for each sample was calculated according to the following formula:

$$\text{Hemolysis rate (\%)} = (D0 - D2)/(D1 - D2) \times 100\%,$$

where $D0$ is the absorbance of the sample.

2.7 Endothelial cell growth behavior

2.7.1 Cell adhesion

The sterilized samples were firstly placed in a 24-well culture plate. Nearly 0.5 mL endothelial cell (ECV304) suspension (5×10^4 cells/mL) and 1.5 mL medium

(DMEM) were successively added to each sample. After being incubated 1 and 3 days at 37°C in a humidified atmosphere containing 5% CO_2, respectively, the samples were washed three times by PBS, and then the adhered cells were fixed 3 h by 2.5% glutaraldehyde at 4°C. 200 μL rhodamine (10 μg/mL in PBS) was added to the surface of each sample for 30 min, and then the sample was washed twice with PBS. Afterward, 200 μL DAPI (500 ng/mL in PBS) was added to the stain for 8 min, and then the sample was washed twice with PBS. Finally, the stained sample was observed away from light using fluorescence microscopy (Zeiss, invertedA2).

2.7.2 Endothelial cell proliferation

Endothelial cells (5×10^4 cells/mL) were seeded on the samples and cultured as described above. After being cultured 1 and 3 days, respectively, each sample was added 0.5 mL CCK-8 (Beyotime Biotechnology Co., Ltd, Shanghai, China) solution (CCK-8:medium = 9:1) and then incubated 3.5 h at 37°C. Subsequently, 200 μL supernatant was transferred to a 96-well plate, and the proliferation activity of endothelial cells was evaluated by measuring the absorbance at 450 nm with a microplate reader (Bio-Tek, Eons).

2.7.3 Determination of nitric oxide (NO) activity of the endothelial cells

NO release from the endothelial cells was measured by the Griess method. The Griess Reagent I and II (Beyotime Biotechnology Co., Ltd, Shanghai, China) were firstly restored to room temperature and the standard samples were prepared at the same time. The endothelial cells were cultured on the sample surface for 1 and 3 days, respectively. 50 μL cell supernatant was added into a 96-well plate. Then, 50 μL of Griess Reagent I and II were added in turn. Finally, the OD value was measured at 540 nm with a microplate reader (Bio-Tek, Eons), and the NO concentration was calculated according to the standard curve.

2.7.4 Expression of vascular endothelial growth factor (VEGF)

The VEGF expression of the endothelial cells was measured by ELISA (Beyotime Biotechnology Co., Ltd, Shanghai, China). The endothelial cells were cultured on the sample surface for 1 and 3 days, respectively. The endothelial cell culture supernatant was taken out to dilute five times and then added to the bottom of the enzyme label plate. After being cultured for 30 min at 37°C, the enzyme label plate was washed five times with PBS. About 100 μL of horseradish peroxidase (HRP) enzyme agent was added to each hole to incubate for 60 min at 37°C. After the samples were washed five times, 50 μL chromogenic agents A and B were added into each hole in turn. The samples were kept away from light for 15 min at 37°C. Finally, the termination solution was added to terminate the reaction. The OD value was measured at 450 nm with a microplate reader (Bio-Tek, Eons), and the concentration of VEGF was calculated according to the standard curve.

2.8 Statistical analysis

For the analysis of water contact angle, protein adsorption, ions release, GMP140, HR, endothelial cell proliferation, NO, and VEGF expression, three parallel samples were measured, the values were averaged and expressed as mean ± standard derivation (SD). The results were statistically analyzed by SPSS software using one-way analysis of variance, and $p < 0.05$ is considered to be statistically significant.

3 Results and discussion

3.1 Sample characterization

Figure 1 shows the SEM images of different samples. The regular nanotube arrays with an inner diameter of about 60 nm and an outer diameter of about 90–110 nm were successfully prepared on the titanium surface after anodization. After annealing at 450°C, the diameter of the nanotubes could expand outward by about 5–10 nm, and the tube wall became thicker, but the overall morphologies of TNTA remained unchanged. Some studies have shown that the TNTA could be transformed into anatase crystal [18], which has a larger volume, resulting in the outward expansion of the nanotubes. In addition, the anatase TiO_2 can also be gradually integrated into the nanotube wall by forming large microcrystals, leading to the expansion of the nanotube structure and rougher surface [19]. After the deposition of polydopamine on the surface, the inner diameter of TNTA–Dopa nanotubes decreased slightly and

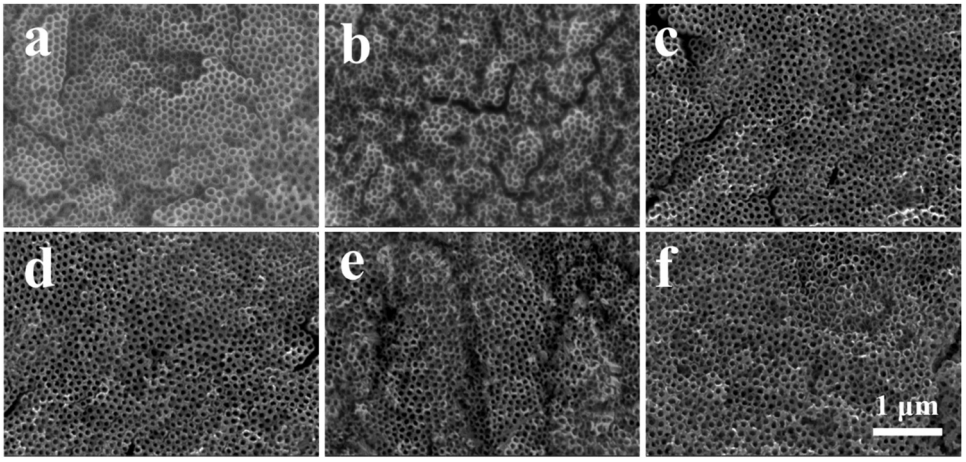

Figure 1: Surface morphologies of (a) TNT, (b) TNTA, (c) TNTA–Dopa, (d) TNTA–Dopa–Cu–Sr0.5, (e) TNTA–Dopa–Cu–Sr1, and (f) TNTA–Dopa–Cu–Sr2.

the wall thickness increased, but the regular nanotube array structure was not changed. After the incorporation of Cu^{2+} and Sr^{2+}, the surface tubular structure did not change significantly, but the wall thickness and the surface roughness of the nanotubes further increased, and the inner diameter of the nanotube decreased by 5–10 nm, suggesting that Cu^{2+} and Sr^{2+} were successfully incorporated into the nanotubes *via* the chelation of dopamine.

Figure 2 is the cross-sectional view and the main element distribution maps of the different samples, and Table 1 shows the element amounts of the different samples. The length of the nanotube was about 4–6 μm measured by the cross-sectional view. The results of element distribution maps showed that the elements were evenly distributed in the nanotube wall. After the anodization, a large number of O elements appeared on TNT, which was

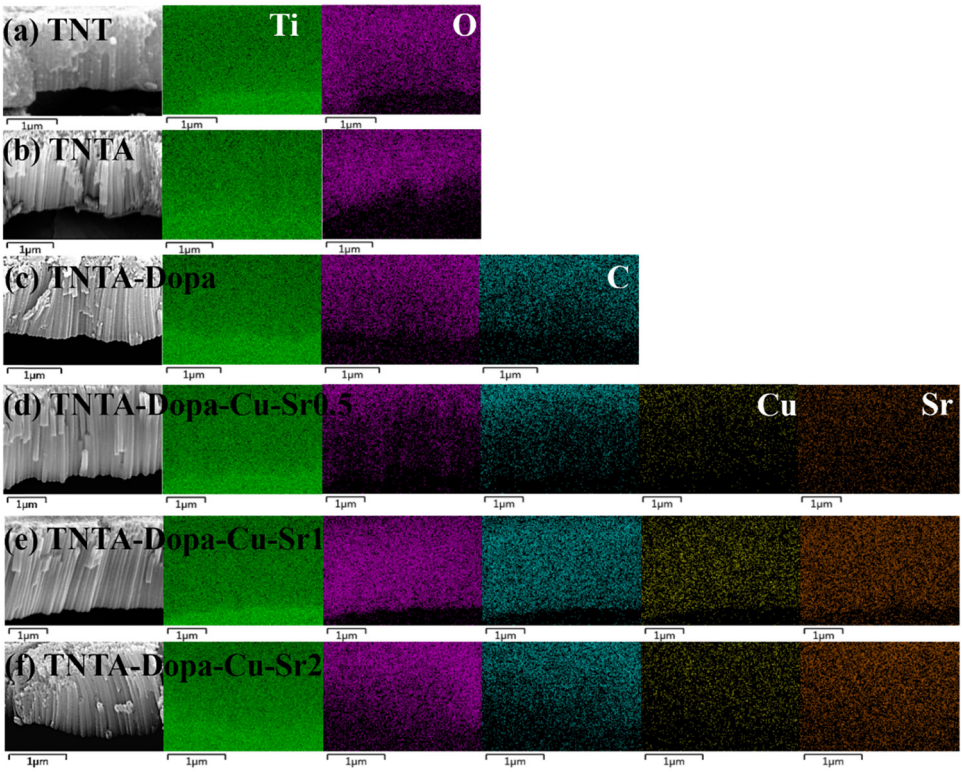

Figure 2: Cross-section morphologies and elements mapping of TNT (a), TNTA (b), TNTA-Dopa (c), TNTA-Dopa-Cu-Sr0.5 (d), TNTA-Dopa-Cu-Sr1 (e), TNTA-Dopa-Cu-Sr2 (f)

Table 1: The element concentrations (wt%) of the different samples characterized by EDS

Element	Ti	O	F	C	Cu	Sr
TNT	64.4	25.3	10.3	—	—	—
TNTA	58.9	40.6	0.5	—	—	—
TNTA–Dopa	48.2	37.8	0.4	13.6	—	—
TNTA–Dopa–Cu–Sr 0.5	47.6	31.3	0	19.8	0.2	1.3
TNTA–Dopa–Cu–Sr 1	48.0	33.2	0	14.8	1.2	2.8
TNTA–Dopa–Cu–Sr 2	54.4	31.3	0	10.3	0.5	3.6

mainly due to the formation of oxides on the surface. After annealing treatment, the amount of oxygen increased greatly because of aerobic treatment. At the same time, the F element almost disappeared. After the polydopamine coating was prepared on the surface of TNT, a C element could be detected on the TNTA–Dopa surface, indicating that the polydopamine coating was successfully introduced on the surface and inside the nanotubes. After loading different amounts of Cu^{2+} and $Sr^{2+,}$ there were different contents of Cu^{2+} and Sr^{2+} in TNTA–Dopa–Cu–Sr0.5, TNTA–Dopa–Cu–Sr1, and TNTA–Dopa–Cu–Sr2 nanotubes. At the same time, the content of Sr^{2+} increased with the increase of Cu/Sr ratio, which proved that Cu^{2+} and Sr^{2+} were successfully loaded into the nanotubes.

Figure 3 shows the XRD patterns of the different samples. It can be seen that no new diffraction peaks were found on the Ti surface beside the titanium peak. Compared with the titanium alloy, the diffraction pattern after the anodization had hardly been changed with only peaks of Ti matrix, suggesting that no new crystalline phase was formed during the anodizing process. It has been reported that the oxide layer on the titanium surface is semi-crystalline, while the synthesized TNT are amorphous [20]. After annealing treatment at 450°C, in addition to the diffraction peaks of Ti, the diffraction peaks of anatase TiO_2(101), (103), (004), (200), (105), (211), and (116) appeared at 2θ = 25.37, 37.88, 38.61, 48.10, 53.90, 55.10 and 68.76, respectively, indicating that the annealing treatment can change the surface crystal structure of the nanotube arrays and new crystal phases appeared. The formation of a new phase had a significant influence on the properties and functions of materials [21,22]. After Cu^{2+} and Sr^{2+} loaded, the crystal structure was not affected obviously.

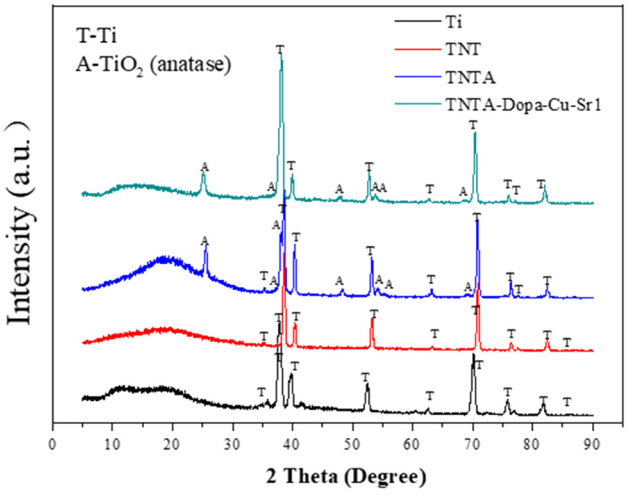

Figure 3: XRD of pure Ti, TNT, TNTA, and TNTA–Dopa–Cu–Sr1.

For determining the release profiles of Cu and Sr ions, the TNTA–Dopa–Cu–Sr samples were immersed in PBS solution for different times, and Cu^{2+} ions and Sr^{2+} were collected to measure the release curves. The release profiles of Cu and Sr ions are shown in Figure 4. According to the literature, the concentration of Sr^{2+} at 2–8 mg/L can promote endothelial cell viability, proliferation, and adhesion [14]. It can be seen that the content of Sr^{2+} released in this study was within the range of cell physiological concentration. In general, for both the Cu and Sr ions, the release amounts had a burst release behavior on the first day. The release amounts of two ions decreased slowly and became steady after 1 day. The larger the loaded ion amount was, the faster the ion was released. Moreover, the release rate of Sr^{2+} was significantly higher than that of $Cu^{2+,}$ which can be attributed to the fact that the dopamine coating containing Sr^{2+} was exposed to the outer surface. After the first week, the release of ions entered a stage of slow increase. After that, there would be a stable release lasting until 14 days, indicating that the ions from the samples could release over 14 days.

3.2 Surface hydrophilicity and protein adsorption

Generally speaking, the hydrophilic surface can adsorb a large number of water molecules to reduce the nonspecific protein adsorption and further prevent platelet adhesion, which can improve the anticoagulant performance [23]. To clarify the relationship between the surface morphology and the biocompatibility of TNT, its hydrophilicity/hydrophobicity was studied by measuring the water contact angle, and the adsorption of two main proteins (albumin and FIB) in human blood was characterized by the BCA method.

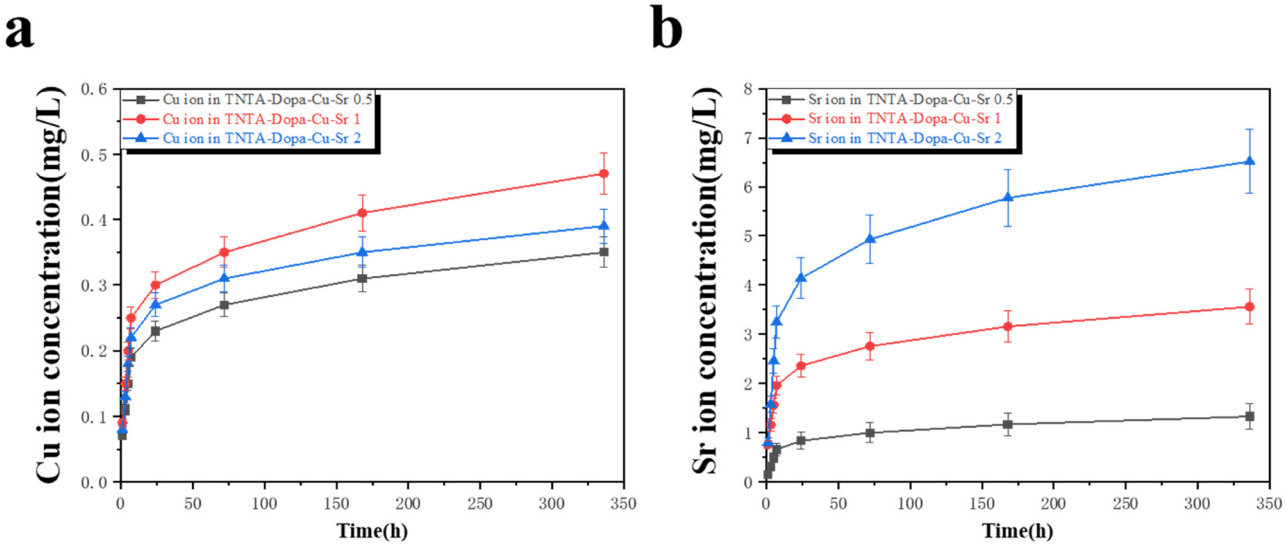

Figure 4: Cu (a) and Sr (b) ions release profiles in PBS for 14 days.

Figure 5a shows the water contact angle results of the different samples. After anodization, a layer of porous TNT could be produced on the titanium surface. The hollow nanotubular structure not only increased the surface roughness but also can accommodate water to some degree. At the same time, a large number of hydrophilic oxygen atoms were introduced on the surface and inside of the nanotubes after the anodization. Therefore, TNT showed good hydrophilicity. Some reports have shown that the annealing treatment can remove organic pollutants and enhance the hydrophilicity of the TiO_2 surface [24,25]. And the increase of the surface roughness will reduce the contact angle and affect the wettability by increasing the critical surface tension [26]. After annealing treatment, the hydrophobic fluorine element almost disappeared and the diameter of TNT expanded outward as well as the roughness increased. In addition, as shown in Figure 3, the amorphous TiO_2 can be transformed into the anatase crystal structure after annealing treatment which has better hydrophilicity than amorphous TNT [27]. Consequently, the hydrophilicity of TNTA was further improved. The preparation of polydopamine introduced amine groups on the surface, which can form hydrogen bonds with water molecules to further improve hydrophilicity [28]. When the polydopamine coating was fabricated on the surface of TNT, the surface hydrophilicity further increased. On one hand, the Cu^{2+} and Sr^{2+} were loaded in the hydrophilic polydopamine coating. On the other hand, after Cu^{2+} and Sr^{2+} were loaded, the sample surface became rougher. Therefore, the hydrophilicity of the samples loaded with Cu^{2+} and Sr^{2+} was improved, especially the water contact angle of TNTA–Dopa–Cu–Sr1 was less than 5°, indicating that it had super hydrophilicity.

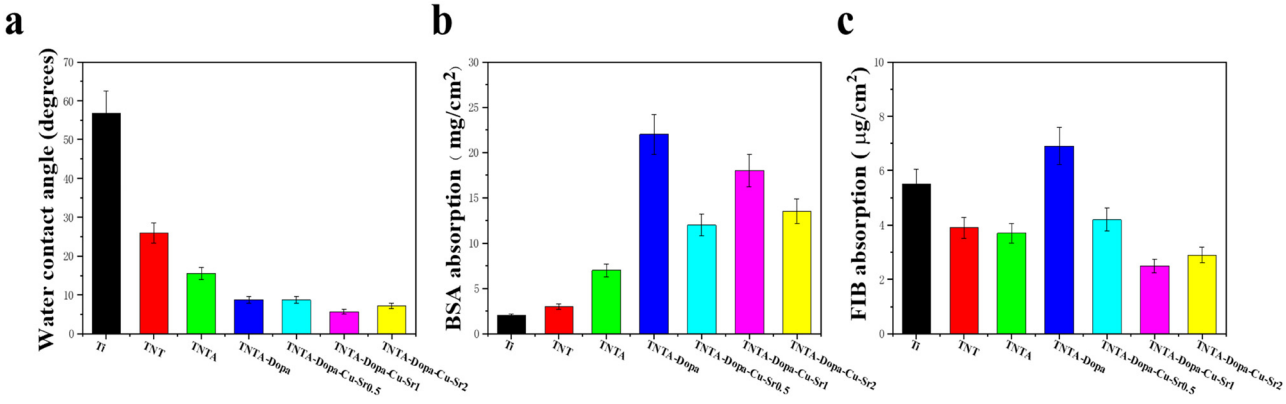

Figure 5: (a) Water contact angle, (b) BSA absorption, and (c) FIB absorption of the different samples.

The adsorption concentrations of BSA and FIB on the different surfaces are shown in Figure 5b and c, respectively. Generally speaking, when biomaterials are implanted into the human body, proteins will be firstly adsorbed on the surface. Additionally, competitive adsorption, desorption, and rearrangement will occur. These behaviors of proteins further determine the adhesion behavior and activation state of the platelets in the blood and affect blood compatibility [29]. By and large, albumin adsorption can reduce the platelet adhesion and thus inhibit the occurrence of coagulation and prolong the coagulation time [30]. On the contrary, FIB adsorption can deteriorate the blood compatibility of biomaterials [31]. It was also found that the shape of protein may affect adsorption [32]. The small size and heart shape of albumin make it easy to pass through a stable water layer near the surface. However, FIB is stretched and cannot easily attach to the hydrophilic surface. For hydrophobic surfaces, the water layer is weakened, which helps FIB diffuse to the surface and adjust its direction. Therefore, albumin tends to be adsorbed on the hydrophilic surface, while FIB tends to be adsorbed on the hydrophobic surface [32].

As shown in Figure 5b, due to the hydrophobicity of the blank pure titanium, the BSA protein adsorption was very low. The specific surface area and surface hydrophilicity increased significantly after the anodic oxidation, which is conducive to the adsorption of albumin [33]. Moreover, protein adsorption also depends on the surface charge characteristics of materials and proteins, and the electrostatic interaction between BSA and TNT may promote or inhibit protein adsorption [34]. This study has also shown that TNT are negatively charged [35], which can promote the adsorption of the positively charged BSA. Therefore, when titanium was anodized to form a TiO_2 nanotube structure, the content of BSA adsorbed on the surface increased. After annealing treatment, the content of FIB protein adsorbed on the surface was significantly reduced while the adsorption capacity of BSA was increased. This was because the increase of surface roughness, hydrophilicity, and the change of crystal structure further enhanced the albumin adsorption and weakened the adsorption performance of FIB. There was competitive adsorption between albumin and FIB. After the polydopamine coating was prepared on the surface, the adhesion of dopamine can significantly increase the content of BSA and FIB adsorbed on the surface [36]. The chelation of Cu^{2+} and Sr^{2+} made the tube wall thicker, but the thicker tube wall has a weak effect on the protein accumulation [37]. The adsorption capacity of BSA was reduced as compared to TNTA–Dopa. However, after Cu^{2+} and Sr^{2+} were loaded, the hydrophilicity was significantly improved when compared with TNTA, leading to the enhancement of BSA adsorption. The competitive adsorption of albumin and FIB was particularly obvious for Cu and Sr ions incorporated nanotubes. Among them, TNTA-Dopa–Cu–Sr1 had the best hydrophilicity, the most BSA protein adsorption, and the lowest FIB protein adsorption can occur on the surface, which may make the material have the best blood compatibility.

3.3 Blood compatibility

Platelet adhesion is one of the important methods to evaluate blood compatibility. Platelets can promote blood coagulation through adhesion, aggregation, and release of other components. Therefore, the materials with good blood compatibility should have the ability to inhibit platelet adhesion and activation [29]. Studies have shown that the adsorbed albumin can inhibit platelet adhesion, while the adsorbed FIB will promote platelet adhesion and activation [38]. As shown in Figure 6a and b, it can be seen that the number of the platelets adhered to the titanium surface was relatively large and the attached platelets spread obviously, indicating that the platelets on the blank titanium surface had been activated and the blood compatibility was limited. After the anodization, the number of the attached platelets decreased significantly, because the surface of TNT can inhibit the adhesion of platelets by reducing the FIB adsorption. After annealing treatment, the platelet adhesion did not change significantly. After the deposition of dopamine coating, platelet adhesion increased significantly because dopamine was oxidized and polymerized to form a layer of polydopamine (Dopa). The disadvantage of Dopa layers is that they usually strongly adsorb proteins. As shown in Figure 5b and c, the content of albumin and FIB significantly increased on TNTA–Dopa. Therefore, Dopamine coating must be completely covered by the bioactive substances to avoid nonspecific adsorption [39]. After the incorporation of Cu^{2+} and Sr^{2+}, the number of platelet adhesion decreased significantly, and the trend of decreasing platelet adhesion of TNTA-Dopa–Cu–Sr1 was the most obvious. On one hand, Cu can reduce platelet aggregation through collagen [40]. On the other hand, with the increase of Sr^{2+} concentration, albumin adsorption increased and FIB adsorption decreased, which also contributed to reducing the adhesion of platelets.

The GMP140 expression can be used to judge the degree of platelet activation. The more the platelets

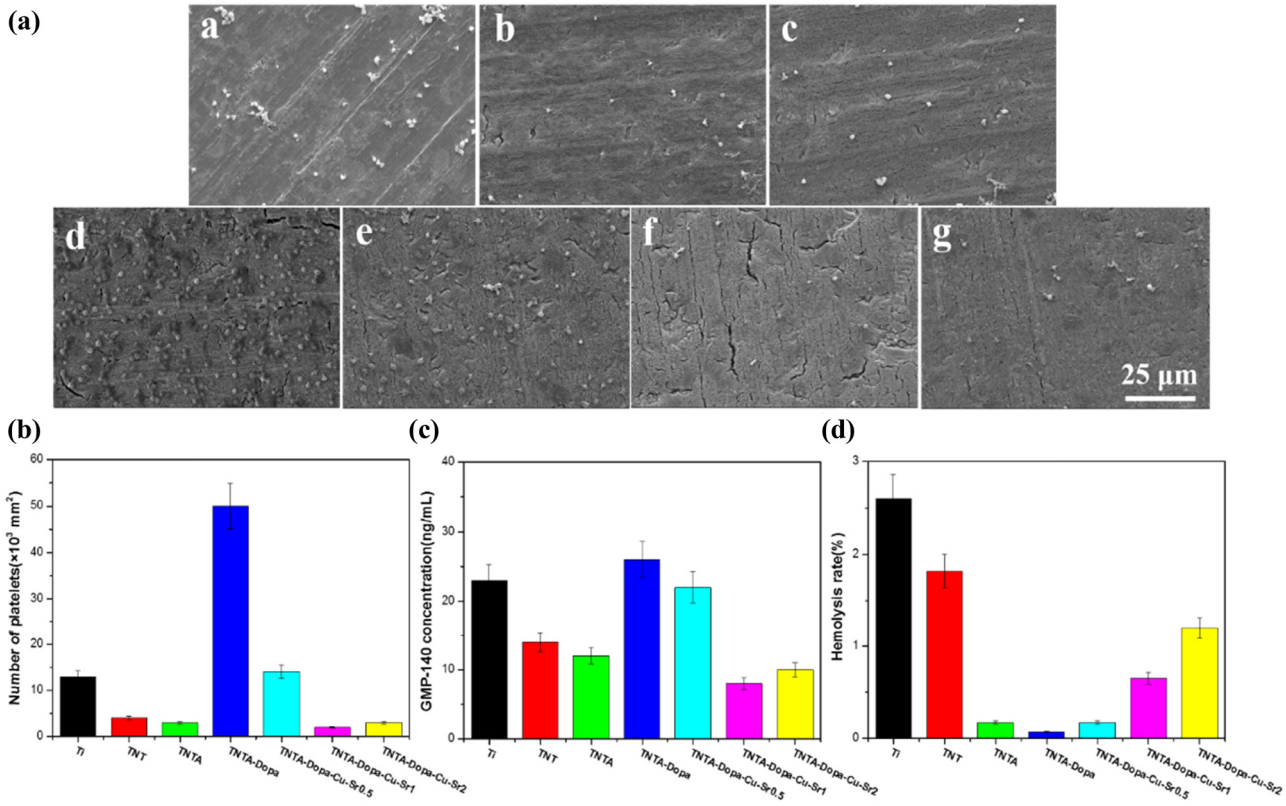

Figure 6: (a) SEM images of platelets adhered on the surface of pure Ti (a), TNT (b), TNTA (c), TNTA–Dopa (d), TNTA–Dopa–Cu–Sr0.5 (e), TNTA–Dopa–Cu–Sr1 (f), TNTA–Dopa–Cu–Sr2 (g)); (b) the number of the platelets on the different samples; and (c) and (d) are the results of GMP140 and the hemolysis rate for the different samples, respectively.

adhere, the more content of GMP140 can be detected, leading to form the thrombosis [41]. Figure 6c shows the GMP140 results of the different samples. It can be seen that the platelets were highly activated on the pristine titanium surface, which is easy to induce human blood coagulation. After the anodic oxidation, the TNT were formed so that the platelet adhesion and activation were significantly reduced. The TNTA had good blood compatibility, which was the same as TNT. After the polydopamine deposition, platelet adhesion increased sharply due to its high viscosity and the content of platelet activation also increased significantly. It has been found that FIB deposition on the surface of platelet membrane-binding receptors will lead to platelet activation and plasma coagulation [42]. After Cu^{2+} and Sr^{2+} were loaded, the amount of FIB adhesion decreased with the increase of Sr^{2+}, resulting in the decrease of platelet adhesion and activation. The GMP140 value for TNTA-Dopa–Cu–Sr1 was the smallest, indicating that the amount of FIB adsorption and platelet adhesion were positively correlated with platelet activation.

To further study the effects of the different materials on red blood cells, HR was also measured. HR is one of the important factors to characterize the interaction between biomaterials and erythrocytes. According to the international standard (ISO10993-4), the HR below 5% means that the material meets the requirements of HR. If the measured HR is more than 5%, the material is not suitable for use as a blood-contacting biomaterial [43]. Hemolysis can affect thrombosis by affecting coagulation and other processes [44,45]. Figure 6d shows the HR of the different samples. It can be seen that the HR of all samples was less than 5%, indicating that none of them can cause serious hemolysis. Studies have shown that the increase of hydrophilicity can lead to higher hemolytic activity [46], but some studies have shown that the increase of hydrophobicity can lead to higher hemolytic activity [47]. As shown in Figure 6d, the surface of TNT had good hydrophilicity and a lower HR than the pure titanium, which could improve blood compatibility. After annealing treatment, the hydrophilicity increased and the HR decreased again. After the construction of polydopamine

coating, the hydrophilicity increased again and the HR decreased. It can be considered that hydrophobic materials are more likely to cause higher HR. However, when Cu^{2+} and Sr^{2+} were loaded, the results were reversed and the HR was improved. The hydrophilic materials may lead to higher HR. Therefore, the hemolytic property of the material can't be judged only from the hydrophilicity and hydrophobicity. The hemolytic property is not only related to the hydrophilicity/hydrophobicity but also related to the chemical composition, morphology, and structure of the surface. With the increased content of Sr^{2+}, the HR was higher than that of TNTA. In addition, due to the reason that the surface was too rough and the large release of Sr^{2+} in a short time, it can result in the rupture of some red blood cells and then lead to higher HR.

3.4 Endothelial cell growth behaviors

Endothelial cells control the angiogenesis of each organ system and participate in regulating nutrients, various bioactive molecules, and the flow of the blood cells. Generally speaking, cells will change their morphologies after contact with biomaterials to realize the integration of materials and cells. The whole process of cell adhesion and diffusion includes cell adhesion, filamentous pseudopodia growth, cytoplasmic reticular structure change, flattening of cell clusters, and surrounding cytoplasmic folding [48]. Cell adhesion is widely used to investigate cell behaviors. In this study, the cell adhesion behavior was first studied by cell fluorescence staining. Figure 7 is the fluorescent images of the endothelial cells adhered to the surfaces of the different samples. It can be seen that the number of cells adhered on the blank titanium surface was few and the adhered endothelial cells were mainly circular, indicating that the cells did not grow well on the surface. The number of endothelial cell adhesion decreased after the anodic oxidation. This is because the thickness and diameter of the nanotubes have an important effect on cell behavior. Nanotube thickness can affect cell behavior through any form of surface leaching (such as fluoride in the structure) and the chemical accumulation effects [49]. Due to the reduction of cytotoxic fluoride ions on the surface, the number of cell adhesion decreased after the anodization, but the morphology of cells began to spread. This is because OH^- and F^- in the anodizing electrolyte solution were adsorbed on the surface of TNT during the anodization. The negatively charged nanotubes could attract the positively charged

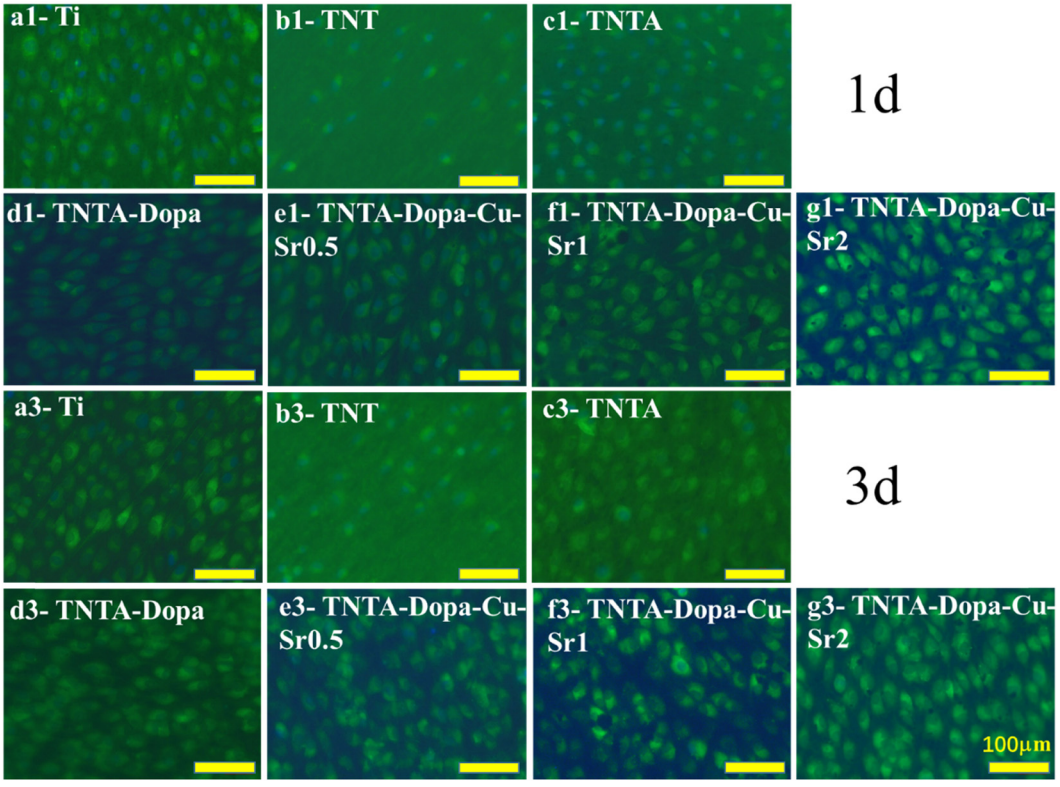

Figure 7: The fluorescent images of the endothelial cells adhered to the different samples.

proteins to improve cell adhesion [50]. After annealing treatment, the hydrophilicity and the surface area of TNTA were increased due to the increase of roughness. At the same time, the fluorine ions were greatly reduced, so the cells adhered to the surface were significantly increased and most of them were spread. When the polydopamine coating was formed on the surface, the surface became super hydrophilic. Studies have shown that hydrophilic surfaces interact closely with the biological fluids to promote protein adsorption and subsequent interaction with the cell receptors [51]. Moreover, dopamine coating has a certain viscosity, which can make cells adhere more easily on the surface, therefore, the number of endothelial cells adhered to TNTA–Dopa surface increased significantly. Sr is an essential micronutrient affecting many aspects of human health. The homeostasis of Sr^{2+} in cells is very important for cell function and survival. McAuslan and Gole [52] first reported that micromolar $CuSO_4$ can induce angiogenesis in rabbits, and Cu^{2+} can attract endothelial cells to migrate and form new capillaries [53]. Therefore, after Cu^{2+} and Sr^{2+} were loaded, the cell adhesion was improved. With the increase of Sr^{2+} concentration, more and more endothelial cells adhered to the surface and most of them were spreading, indicating that TNTA-Dopa–Cu–Sr can promote the growth of endothelial cells.

Endothelial cell proliferation also affects re-endothelialization after the implantation. Rapid endothelialization on the surface contributes to preventing intimal hyperplasia and restenosis after vascular stent implantation [54]. To further study the proliferation of endothelial cells on the surface of TNT loaded with Cu^{2+} and Sr^{2+}, endothelial cells were cultured with samples for 1 day and 3 days, respectively, and CCK-8 was tested and the results are shown in Figure 8a. It can be seen that the proliferation of the endothelial cells on the surface of titanium alloy was restricted. When the titanium alloy was anodized, the proliferation of the endothelial cells on the surface was improved. This was because the surface of TNT can adsorb more nutrients, thus promoting the proliferation of endothelial cells. In general, endothelial cells are more likely to adhere to hydrophilic surfaces. After annealing treatment, the surface of TNTA samples showed super hydrophilicity, so the proliferation of endothelial cells on the TNTA surface was more obvious. When dopamine was polymerized on the surface, the hydroxyl and amine groups on the surface further increased, and the cells could adhere to these functional surfaces through nonreceptor-binding force (electrostatic interaction), to promote cell proliferation. After loading Cu^{2+} and Sr^{2+}, the cells further proliferated. With the increase of Sr concentration, the proliferation was more obvious, indicating that the loading of Cu^{2+} ions could promote the growth of endothelial cells and the loading of Sr^{2+} could further promote cell proliferation.

VEGF is a highly specific vascular endothelial growth factor. It can induce angiogenesis *in vivo* and promote vascular permeability, extracellular matrix deformation, vascular endothelial cell migration, and proliferation [55]. Normal endothelial cells will express a certain amount of VEGF, and its normal expression can further promote the growth of endothelial cells. Therefore, the study of VEGF expression is of great significance to evaluate the function of endothelial cells. As shown in Figure 8b, the VEGF expression of the anodized TNT was higher than that of pure titanium because the number of endothelial cell adhesion increased significantly. VEGF is one of the substances secreted by the normal endothelial cells, which plays an important role in maintaining normal physiological function and cell proliferation. The increase of VEGF

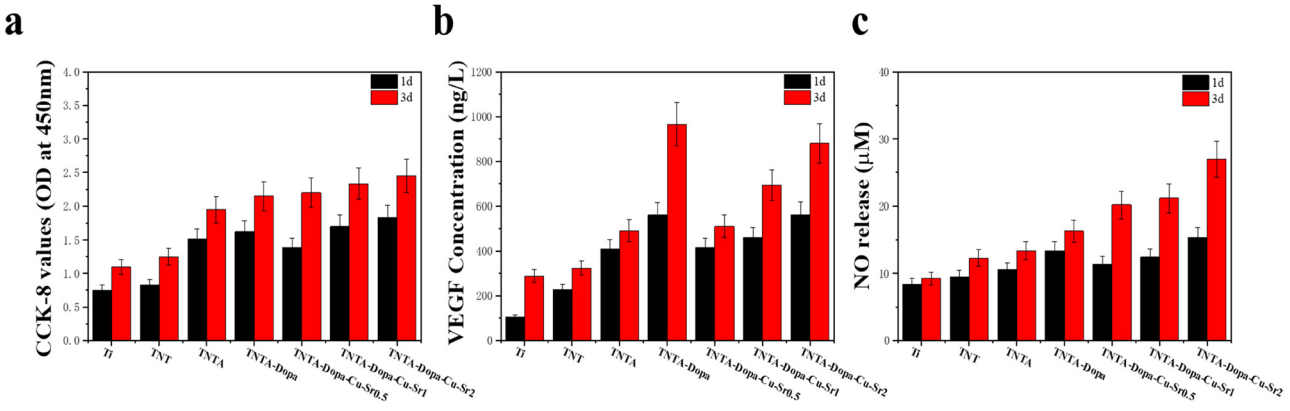

Figure 8: CCK-8 values (a), VEGF (b), and NO (c) activities of the endothelial cells grown on the different samples surfaces for 1 and 3 days, respectively.

expression indicates a normal function of endothelial cells. When the polydopamine coating was prepared on the surface, due to the good biocompatibility of dopamine, it was conducive to the growth and function expression of the endothelial cells, and thus the endothelial cells would release more VEGF. After loading Cu^{2+} and Sr^{2+}, the expression of VEGF increased again because Cu^{2+} can upregulate VEGF gene expression by affecting the regulator hypoxia-inducible factor 1 to stimulate endothelial cells [11,56]. Studies have shown that Sr coating can also promote angiogenesis, VEGF release, and angiogenesis gene expression [57]. As shown in Figure 8b, the expression of VEGF increased with the increase of Sr^{2+}.

The NO production is one of the key physiological functions of the endothelial cells. NO plays many key roles in the vascular system. It can maintain the hemostasis of the blood vessels, act as an effective vasodilator, regulate the proliferation and migration of endothelial cells and inhibit the formation of thrombosis [58]. Figure 8c shows the NO secretion of endothelial cells growing on the different samples' surfaces. It can be seen that the endothelial cells on the TiO_2 nanotube surface released more NO than pure titanium, which was related to the TiO_2 nanotube's excellent biocompatibility. The TNT can stimulate endothelial cell growth and VEGF expression, which can activate the production of eNOS in endothelial cells by mediating protein kinase, to increase the release of NO. The TNTA promoted the growth of endothelial cells, so they released more NO after the annealing treatment. When the polydopamine coating was further prepared on the surface, the released NO was also larger due to the large number of endothelial cells growing on the TNTA–Dopa surface. Studies have shown that the addition of Cu^{2+} will not only promote the release of NO [12] and help to improve endothelial cell function, but also maintain normal vasodilation and contribute to reducing the risk of acute thrombosis after stent implantation [59]. A certain concentration of Sr can promote the proliferation of vascular endothelial cells. By affecting the secretion of endothelin and NO, Sr can reduce vascular tension [14]. Therefore, when Cu^{2+} and Sr^{2+} were released from the sample surfaces, the NO release was also increased.

4 Conclusion

The regular TNT arrays were successfully prepared on the titanium surface by anodic oxidation. After annealing treatment, the amorphous TNT changed into an anatase crystal structure, which significantly affected the properties of the titanium surface. The loading of Cu^{2+} and Sr^{2+} *via* dopamine on the surface of TNT can not only significantly improve the hydrophilicity but also promote albumin adsorption and inhibit FIB adsorption (especially TNTA–Dopa–Cu–Sr1), showing a selective adsorption effect between albumin and FIB. At the same time, loading Cu and Sr ions can not only reduce platelet adhesion and activation, but also promote the adhesion, proliferation, and functional expression of endothelial cells. Therefore, the method of this study can be used for the surface modification of the blood-contacting titanium-based biomaterials to simultaneously improve blood compatibility and promote the growth of endothelial cells, which can be further used in implantable medical devices such as vascular stents.

Funding information: This work was financially supported by the National Natural Science Foundation of China (31870952), Natural Science Foundation of Jiangsu Province of China (BK20181480) and Innovation Project of Huaiyin Institute of Technology (HGYK202107).

Author contributions: All authors have accepted responsibility for the entire content of this manuscript and approved its submission.

Conflict of interest: The authors state no conflict of interest.

References

[1] Im E, Lee SY, Hong SJ, Ahn CM, Kim JS, Kim BK, et al. Impact of late stent malapposition after drug-eluting stent implantation on long-term clinical outcomes. Atherosclerosis. 2019;288:118–23. doi: 10.1016/j.atherosclerosis.2019.07.014.

[2] Manivasagam VK, Popat KC. In vitro investigation of hemocompatibility of hydrothermally treated titanium and titanium alloy surfaces. ACS Omega. 2020;5:8108–20. doi: 10.1021/acsomega.0c00281.

[3] Jin Z, Yan X, Liu G, Lai M. Fibronectin modified TiO_2 nanotubes modulate endothelial cell behavior. J Biomater Appl. 2018;33:44–51. doi: 10.1177/0885328218774512.

[4] Shahramian K, Abdulmajeed A, Kangasniemi I, Söderling E, Närhi T. TiO_2 coating and UV photofunctionalization enhance blood coagulation on zirconia surfaces. BioMed Res Int. 2019;2019:8078230. doi: 10.1155/2019/8078230.

[5] Tan AW, Murphy BP, Ahmad R, Akbar SA. Review of titania nanotubes: Fabrication and cellular response. Ceram Int. 2012;38:4421–35. doi: 10.1016/j.ceramint.2012.03.002.

[6] Qiao H, Xiao H, Huang Y, Yuan C, Zhang X, Bu X, et al. SiO_2 loading into polydopamine-functionalized TiO_2 nanotubes for biomedical applications. Surf Coat Technol. 2019;364:170–9. doi: 10.1016/j.surfcoat.2019.02.089.
[7] Roguska A, Pisarek M, Belcarz A, Marcon L, Holdynski M, Andrzejczuk M, et al. Improvement of the bio-functional properties of TiO_2 nanotubes. Appl Surf Sci. 2016;388:775–85. doi: 10.1016/j.apsusc.2016.03.128.
[8] Aydın MTA, Hoşgün HL, Dede A, Güven K. Synthesis, characterization and antibacterial activity of silver-doped TiO_2 nanotubes. Spectrochim Acta A. 2018;205:503–7. doi: 10.1016/j.saa.2018.07.063.
[9] Zhang L, Guo J, Huang X, Zhang Y, Han Y. The dual function of Cu-doped TiO_2 coatings on titanium for application in percutaneous implants. J Mater Chem B. 2016;21:3788–800. doi: 10.1039/C6TB00563B.
[10] Matos L, Gouveia A, Almeida H. Copper ability to induce premature senescence in human fibroblasts. GeroScience. 2012;34:783–94. doi: 10.1007/s11357-011-9276-7.
[11] Feng W, Ye F, Xue W, Zhou Z, Kang YJ. Copper regulation of hypoxia-inducible factor-1 activity. Mol Pharmacol. 2009;75:174–82. doi: 10.1124/mol.108.051516.
[12] Demura Y, Ameshima S, Ishizaki T, Okamura S, Miyamori I, Matsukawa S. The activation of eNOS by copper ion (Cu^{2+}) in human pulmonary arterial endothelial cells (HPAEC). Free Radical Bio Med. 1998;25:314–20. doi: 10.1016/S0891-5849(98)00056-2.
[13] Curtis EM, Cooper C, Harvey NC. Cardiovascular safety of calcium, magnesium and strontium: what does the evidence say? Aging Clin Exp Res. 2012;33:479–94. doi: 10.1007/s40520-021-01799-x.
[14] Xing M, Jiang Y, Bi W, Gao L, Zhou YL, Rao SL, et al. Strontium ions protect hearts against myocardial ischemia/reperfusion injury. Sci Adv. 2021;7:eabe0726. doi: 10.1126/sciadv.abe0726.
[15] Zhang W, Cao H, Zhang X, Li G, Chang Q, Zhao J, et al. A strontium-incorporated nanoporous titanium implant surface for rapid osseointegration. Nanoscale. 2016;8:5291–301. doi: 10.1039/C5NR08580B.
[16] Zhao F, Lei B, Li X, Mo Y, Wang R, Chen D, et al. Promoting *in vivo* early angiogenesis with sub-micrometer strontium-contained bioactive microspheres through modulating macrophage phenotypes. Biomaterials. 2018;178:36–47. doi: 10.1016/j.biomaterials.2018.06.004.
[17] Cheng S, Ke J, Yao M, Shao H, Zhou J, Wang M, et al. Improved osteointegration and angiogenesis of strontium-incorporated 3D-printed tantalum scaffold *via* bioinspired polydopamine coating. J Mater Sci Technol. 2021;69:106–18. doi: 10.1016/j.jmst.2020.08.017.
[18] Gong Z, Hu Y, Gao F, Quan L, Liu T, Gong T, et al. Effects of diameters and crystals of titanium dioxide nanotube arrays on blood compatibility and endothelial cell behaviors. Colloids Surf B. 2019;184:110521. doi: 10.1016/j.colsurfb.2019.110521.
[19] Sun Y, Sun S, Liao X, Wen J, Yin G, Pu X, et al. Effect of heat treatment on surface hydrophilicity-retaining ability of titanium dioxide nanotubes. Appl Surf Sci. 2018;440:440–7. doi: 10.1016/j.apsusc.2018.01.136.
[20] Nguyen QAS, Bhargava YV, Radmilovic VR, Devine TM. Structural study of electrochemically synthesized TiO_2 nanotubes *via* cross-sectional and high-resolution TEM. Electrochim Acta. 2009;54:4340–4. doi: 10.1016/j.electacta.2009.03.034.
[21] Zhou Z, Yu Y, Ding Z, Zuo M, Jing C. Modulating high-index facets on anatase TiO_2. Eur J Inorg Chem. 2018;6:683–93. doi: 10.1002/ejic.201701027.
[22] Asgharizadeh S, Khorram S, Lazemi M, Hosseinzadeha A, Malfois M. Size-dependent interaction of plasma with anatase TiO_2 nanoparticles. Phys Chem Chem Phy. 2020;22:17365–74. doi: 10.1039/D0CP02452J.
[23] Toffoli A, Parisi L, Bianchi MG, Lumetti S, Bussolati O, Macaluso GM. Thermal treatment to increase titanium wettability induces selective proteins adsorption from blood serum thus affecting osteoblasts adhesion. Mater Sci Eng C. 2020;107:110250. doi: 10.1016/j.msec.2019.110250.
[24] Chen J, Zhao A, Chen H, Liao Y, Yang P, Sun H, et al. The effect of full/partial UV-irradiation of TiO_2 films on altering the behavior of fibrinogen and platelets. Colloids Surf B. 2014;122:709–18. doi: 10.1016/j.colsurfb.2014.08.004.
[25] Lorenzetti M, Bernardini G, Luxbacher T, Santucci A, Kobe S, Novak S. Surface properties of nanocrystalline TiO_2 coatings in relation to the in vitro plasma protein adsorption. Biomed Mater. 2015;10:045012. doi: 10.1088/1748-6041/10/4/045012.
[26] Wälivaara B, Aronsson BO, Rodahl M, Lausmaa J, Tengvall P. Titanium with different oxides: in vitro studies of protein adsorption and contact activation. Biomaterials. 1994;15:827–34. doi: 10.1016/0142-9612(94)90038-8.
[27] Varghese OK, Gong D, Paulose M, Grimes CA, Dickey EC. Crystallization and high-temperature structural stability of titanium oxide nanotube arrays. J Mater Res. 2003;18:156–65. doi: 10.1557/jmr.2003.0022.
[28] Qiu WZ, Yang HC, Xu ZK. Dopamine-assisted co-deposition: An emerging and promising strategy for surface modification. Adv Colloid Interface Sci. 2018;256:111–25. doi: 10.1016/j.cis.2018.04.011.
[29] Brash JL, Horbett TA, Latour RA, Tengvall P. The blood compatibility challenge. Part 2: Protein adsorption phenomena governing blood reactivity. Acta Biomater. 2019;94:11–24. doi: 10.1016/j.actbio.2019.06.022.
[30] Yamazoe H, Oyane A, Nashima T, Ito A. Reduced platelet adhesion and blood coagulation on cross-linked albumin films. Mater Sci Eng C. 2010;30:812–16. doi: 10.1016/j.msec.2010.03.015.
[31] Ueda T, Murakami D, Tanaka M. Analysis of interaction between interfacial structure and fibrinogen at blood-compatible polymer/water interface. Front Chem. 2018;6:542. doi: 10.3389/fchem.2018.00542.
[32] Wu X, Wang C, Hao P, He F, Yao Z, Zhang X. Adsorption properties of albumin and fibrinogen on hydrophilic/hydrophobic TiO_2 surfaces: A molecular dynamics study. Colloids Surf B. 2021;207:111994. doi: 10.1016/j.colsurfb.2021.111994.
[33] Nagassa ME, Daw AE, Rowe WG, Carley A, Thomas DW, Moseley R. Optimisation of the hydrogen peroxide pre-treatment of titanium: surface characterisation and protein adsorption. Clin Oral Implant Res. 2008;19:1317–26. doi: 10.1111/j.1600-0501.2008.01611.x.
[34] Fragalà ME, Satriano C. Selective protein adsorption on ZnO thin films for biofunctional nano-platforms. J Nanosci Nanotechnol. 2010;10:5889–93. doi: 10.1166/jnn.2010.2433.

[35] Nasirpouri F, Yousefi I, Moslehifard E, Khalil-Allafi J. Tuning surface morphology and crystallinity of anodic TiO_2 nanotubes and their response to biomimetic bone growth for implant applications. Surf Coat Technol. 2017;315:163–71. doi: 10.1016/j.surfcoat.2017.02.006.
[36] Jia L, Han F, Wang H, Zhu C, Guo Q, Li J, et al. Polydopamine-assisted surface modification for orthopaedic implants. J Orthop Transl. 2019;17:82–95. doi: 10.1016/j.jot.2019.04.001.
[37] Fabre H, Mercier D, Galtayries A, Portet D, Delorme N, Bardeau JF. Impact of hydrophilic and hydrophobic functionalization of flat TiO_2/Ti surfaces on proteins adsorption. Appl Surf Sci. 2018;432:15–21. doi: 10.1016/j.apsusc.2017.08.138.
[38] Tsai WB, Grunkemeier JM, McFarland CD, Horbett TA. Platelet adhesion to polystyrene-based surfaces preadsorbed with plasmas selectively depleted in fibrinogen, fibronectin, vitronectin, or von Willebrand's factor. J Biomed Mater Res. 2002;60:348–59. doi: 10.1002/jbm.10048.
[39] Goh SC, Luan Y, Wang X, Du H, Chau C, Schellhorn HE, et al. Polydopamine-polyethylene glycol-albumin antifouling coatings on multiple substrates. J Mater Chem B. 2018;6:940–9. doi: 10.1039/C7TB02636F.
[40] Assumpção TCF, Ma D, Schwarz A, Reiter K, Santana JM, Andersen JF, et al. Salivary antigen-5/CAP family members are Cu^{2+}-dependent antioxidant enzymes that scavenge O^{2-}. and inhibit collagen-induced platelet aggregation and neutrophil oxidative burst. J Biol Chem. 2013;288:14341–61. doi: 10.1074/jbc.M113.466995.
[41] Hamburger SA, McEver RP. GMP-140 mediates adhesion of stimulated platelets to neutrophils. Blood. 1990;71:550–4. doi: 10.1182/blood.V75.3.550.550.
[42] Xu LC, Bauer JW, Siedlecki CA. Proteins, platelets, and blood coagulation at biomaterial interfaces. Colloids Surf B. 2014;124:49–68. doi: 10.1016/j.colsurfb.2014.09.040.
[43] Liu C, Lin Z, Qiao C, Zhao Z, Wang C, Sun X, et al. Hemocompatibility assay of a micro-catheter using hydrophilic coating biomaterials. Bio-Med Mater Eng. 2018;1:1–9. doi: 10.3233/bme-181028.
[44] Weisel JW, Litvinov RI. Red blood cells: the forgotten player in hemostasis and thrombosis. J Thromb Haemost. 2019;17:271–82. doi: 10.1111/jth.14360.
[45] Bartoli CR, Zhang D, Kang J, Hennessy-Strahs S, Restle D, Howard J, et al. Clinical and in vitro evidence that subclinical hemolysis contributes to LVAD thrombosis. Ann Thorac Surg. 2018;105:807–14. doi: 10.1016/j.athoracsur.2017.05.060.
[46] Kuo ZK, Fang MY, Wu TY, Yang T, Tseng HW, Chen CC, et al. Hydrophilic films: how hydrophilicity affects blood compatibility and cellular compatibility. Adv Poly Technol. 2018;37:1635–42. doi: 10.1002/adv.21820.
[47] Zhang J, Song C, Liu B, Shumei L. The effect of hemolytic activity and protein adsorption of coronary stent with different hydrophobic surface. Heart. 2011;97(21):A77. doi: 10.1136/heartjnl-2011-300867.223.
[48] Hou X, Mao D, Ma H, Ai Y, Zhao X, Deng J, et al. Antibacterial ability of Ag-TiO_2 nanotubes prepared by ion implantation and anodic oxidation. Mater Lett. 2015;161:309–12. doi: 10.1016/j.matlet.2015.08.125.
[49] Pan CJ, Hou YH, Ding HY, Dong YX. Enhancing anticoagulation and endothelial cell proliferation of titanium surface by sequential immobilization of poly(ethylene glycol) and collagen. Appl Surf Sci. 2013;287:443–50. doi: 10.1016/j.apsusc.2013.09.176.
[50] Kabaso D, Gongadze E, Perutková Š, Matschegewski C, Kralj-Iglič V, Beck U, et al. Mechanics and electrostatics of the interactions between osteoblasts and titanium surface. Comput Method Biomec Biomed Eng. 2011;14:469–82. doi: 10.1080/10255842.2010.534986.
[51] Gittens RA, Scheideler L, Rupp F, Hyzy SL, Geis-Gerstorfer J, Schwartz Z, et al. A review on the wettability of dental implant surfaces II: biological and clinical aspects. Acta Biomater. 2014;10:2907–18. doi: 10.1016/j.actbio.2014.03.032.
[52] McAuslan BR, Gole GA. Cellular and molecular mechanisms in angiogenesis. Trans Ophthalmol Soc U K. 1980;100(3):354–58.
[53] McAuslan BR, Reilly W. Endothelial cell phagokinesis in response to specific metal ions. Exp Cell Res. 1980;130:147–57. doi: 10.1016/0014-4827(80)90051-8.
[54] McMullen ME, Bryant PW, Glembotski CC, Vincent PA, Pumiglia KM. Activation of p38 has opposing effects on the proliferation and migration of endothelial cells. J Biol Chem. 2005;280:20995–1003. doi: 10.1074/jbc.M407060200.
[55] Saeko K, Ryoko I, Kazuto H, Atsuhiko H. Adipose-derived stem cells improve tendon repair and prevent ectopic ossification in tendinopathy by inhibiting inflammation and inducing neovascularization in the early stage of tendon healing. Regen Ther. 2020;14:103–10. doi: 10.1016/j.reth.2019.12.003.
[56] Jiang Y, Reynolds C, Xiao C, Feng W, Zhou Z, Rodriguez W, et al. Dietary copper supplementation reverses hypertrophic cardiomyopathy induced by chronic pressure overload in mice. J Exp Med. 2007;204:657–66. doi: 10.1084/jem.20061943.
[57] Yi QQ, Liang PC, Liang DY, Shi JF, Sha S, Chang Q. Multifunction Sr doped microporous coating on pure magnesium of antibacterial, osteogenic and angiogenic activities. Ceram Int. 2021;47:8133–41. doi: 10.1016/j.ceramint.2020.11.168.
[58] Taite LJ, Yang P, Jun HW, West JL. Nitric oxide-releasing polyurethane-PEG copolymer containing the YIGSR peptide promotes endothelialization with decreased platelet adhesion. J Biomed Mater Res B. 2008;84:108–16. doi: 10.1002/jbm.b.30850.
[59] Yue R, Niu J, Li Y, Ke G, Huang H, Pei J, et al. In vitro cytocompatibility, hemocompatibility and antibacterial properties of biodegradable Zn–Cu–Fe alloys for cardiovascular stents applications. Mater Sci Eng C. 2020;113:111007. doi: 10.1016/j.msec.2020.111007.